nature

SUPPLEMENTARY INFORMATION

1. Full methods

2. Sample characteristics

3. Vibram FiveFingers® training study

4. Modelling the collision impulse in different foot strike types

5. Comparison of impact transient data and leg compliance in padded versus unpadded conditions

6 Movies and additional notes

1. Full Methods

Subjects

Five groups of subjects were used (outlined in Table 1 and Supplemental Table 1), including three groups of adults. Group 1: Habitually shod amateur and collegiate athletes from the Harvard University community, recruited by word of mouth, and all habitually shod since early childhood. Group 2: Adult athletes from the Rift Valley Province of Kenya, all training for competition, and recruited by word of mouth in the town of Kapsabet, Kenya; and at Chepkoilel Stadium, Eldoret Kenya. All adult Kenyan subjects were habitually shod, but 75% did not start wearing shoes and training in running shoes until late adolescence. Group 3: Self-identified habitual barefoot runners from the USA, recruited via the internet, who run either barefoot and/or in minimal footwear such as Vibram Five Finger® (VFF) shoes, defined as lacking arch support and cushioning. In addition, two groups of adolescent subjects (aged 11-16) were sampled from two schools in the Rift Valley Province, Kenya. Group 4: A habitually unshod group (N=16; 8 M, 8 F) was recruited from a rural primary school in the Nandi District in which none of children have ever worn shoes (verified by observation and interviews with teachers at the school). Group 5: A habitually shod group (N=16; 9 M, 7 F) was recruited from an urban primary school in Eldoret (Uasin Gishu District) in which all of the children have been habitually shod since early childhood.

For all adults, criteria for inclusion in the study included a minimum of 20 km per week of distance running, and no history of significant injury during the previous 6 months. Habitual barefoot runners were included if they had run either barefoot or in minimal footwear for more than six months, and if more than 66% of their running was either barefoot or in minimal footwear. In order to compare habitual barefoot forefoot strikers (toe-heel-toe runners) and habitually shod rearfoot strikers (heel-toe runners) , kinematic and kinetic data from subsamples of six rearfoot strikers from Group 1 and six forefoot strikers from Group 3 were analyzed in greater depth (see Supplementary Data Table 1).

All information on subject running history was self-reported (with the assistance of teachers for the Kenyan adolescents). All subjects participated on a voluntary basis

and gave their informed consent according to the protocols approved by the Harvard Institutional Review Board, and the Moi University Medical School (for Kenyan subjects). Subjects were not informed about the hypotheses tested prior to recording.

Treatments

All subjects were recorded on flat trackways, approximately 20-25 m long. Subjects in Groups 1-3, and 5 were recorded in barefoot and in running shoes. A neutral running shoe (Asics Gel-Cumulus 10) was provided for Groups 1 and 2, but Groups 3 and 5 ran in their own shoes; subjects in Group 4 were recorded only in the barefoot condition because they had never worn shoes. For Groups 1 and 3, two force plates (see below) were embedded at ground level 80% along the trackway, with a combined force plate length of 1.2 m. Force plates were covered with grip tape (3M Safety Walk, Medium Duty Tread 7741), and runners were asked to practice running prior to recording so that they did not have to modify their stride to strike the plates. Kenyan runners in groups 2, 4,5 were recorded on flat outdoor dirt trackways (with no force plate) that were 20-25 m long, cleaned to remove any pebbles or debris. In all groups, subjects were asked to run at a preferred speed and were given several habituation trials prior to each data collection phase, and they were recorded for 5-7 trials per condition with at least one minute rest between trials to avoid fatigue.

Kinematics

To record angles in lateral view of the ankle, knee, hip, and plantar surface of the foot, a high speed video camera (Fast-Tec Inline 500M, San Diego, CA) was placed approximately 0.5 m above ground level between 2.0 and 3.5 m lateral to the recording region (e.g., the force plate) and recorded at 500 Hz. Circular markers were taped on the posterior calcaneus (at the level of the Achilles tendon insertion), the head of metatarsal V, the lateral malleolus, the joint centre between the lateral femoral epicondyle and the lateral tibial plateau (posterior to Gerdy's tubercle), the midpoint of the thigh between the lateral femoral epicondyle and the greater trochantor of the femur (in Groups 2, 4,5); the greater trochantor of the femur (only in Groups 1 and 3); and the lateral-most point on the anterior superior iliac spine (only in Groups 1 and 3). We were not permitted to place hip and pelvis markers on adolescent Kenyan subjects (Groups 4 and 5). ImageJ

(http://rsb.info.nih.gov/nih-image/) was used to measure three angles in all subjects: (1) the plantar foot angle (PFA), the angle between the earth horizontal and the plantar surface of the foot (calculated using the angle between the lines formed by the posterior calcaneus and fifth metatarsal head markers and the earth horizontal at impact and corrected by the same angle during quiet stance); (2) ankle angle, defined by the fifth metatarsal head, lateral malleolus, and knee markers; (3) knee angle, defined by the line connecting the lateral malleolus and knee and the line connecting the knee and the thigh midpoint (or greater trochantor). Hip angle was also measured in Groups 1 and 2 as the angle between the lateral femoral condyle, the greater trochantor, and the anterior superior iliac spine. All angles were corrected against angles measured during a standing, quiet stance. Average measurement precision, determined by repeated measurements (>5) on the same subjects was ± 0.26°.

Under ideal conditions, PFA angles above 0° indicate a forefoot strike, angles below 0° indicate a rearfoot (heel) strike, and angles of 0° indicate a midfoot strike. However, because of inversion of the foot at impact, lighting conditions and other sources of error, determination of foot strike type was also evaluated by visual examination of the high speed video by three researchers. Note also that ankle angles greater than 0° indicate plantarflexion, and angles less than 0° indicate dorsiflexion.

Additional kinematic data for Groups 1 and 3 were recorded with a 6 camera Qualysis system (ProReflex MCU 240, Qualysis, Gothenburg, Sweden) at 240 Hz. The system was calibrated using a wand with average residuals < 1 mm for all cameras. Four infrared reflective markers were mounted on two 2 cm long balsawood posts, affixed to the heel with two layers of tape following methods described in Ref. 1. An average of these four markers was used to determine foot total and vertical velocity of the foot prior to impact.

Kinetics

Ground reaction forces (GRFs) were recorded in Groups 1 and 3 at 4,800 Hz using AMTI force plates (BP400600, Watertown, MA). All GRFs were normalized to body weight. Traces were not filtered. When a distinct impact transient was present, transient magnitude and the percentage of stance was measured at peak; the rate of loading (ROL) was quantified between 200 N and 90% of the peak (following Ref. 1);

instantaneous ROL was quantified over time intervals of 1.04 ms. When no distinct impact transient was present, the same parameters were measured using the average percentage of stance ±1 standard deviation as determined for each condition in trials with an impact transient.

Effective mass estimation

For Groups 1 and 3, we used equation 2 to estimate the effective mass that generates the impulse at foot landing. The start of the impulse was identified as the instant when the vertical GRF exceeded 4 s.d. of baseline noise above the baseline mean, and the end was chosen to be 90% of the impact transient peak (a "real" time point among rearfoot strike runners, the average of which was used as the end of the transient in FFS runners who lacked a transient); this results in an impulse experienced, on average, through the first 6.2% ± 3.7 s.d. of stance. The integral of vertical GRF over the time period of the impulse is the total impulse and was calculated using trapezoidal numerical integration within the Matlab 7.7 environment using the TRAPZ function (Mathworks Inc., Natick, MA). Three dimensional kinematic data of the foot (see *Kinematics*) were low pass filtered using a 4th order Butterworth filter with a 25 Hz cutoff frequency. The vertical velocity at the moment of impact was found by differentiating the smoothed vertical coordinate (via a piecewise cubic Hermite interpolating polynomial) of the foot using numerical central difference. To minimize the effects of measurement noise, especially because we used differentiated data, we used the average of the three samples immediately prior to impact in calculating the impact velocity. M_{eff} was then estimated as the ratio of the vertical GRF impulse (found by numerical integration) to the vertical impact velocity (found by numerical differentiation).

1. Williams, D. S., McClay, I. S., & Manal, K. T. Lower extremity mechanics in runners with a converted forefoot strike pattern. J Appl. Biomech. **16**, 210-18 (2000).

Supplementary Data 2: Sample characteristics

Supplementary Table 1: Sample characteristics

Group	N (m/f)	Age ±s.d.	Age shod	Height (m) ±s.d.	Weight (kg) ±s.d.	Km run/day ±s.d.
Adults						
1. Habitual shod, USA	8 (6/2)	19.1 ±0.4	<2	1.71 ±0.10	64.4 ±6.7	12.0 ±6.5
2. Transitioned to shod, Kenya	14 (13/1)	23.1 ±3.5	12.4 ±5.6	1.72 ±0.09	55.1 ±6.4	22.0 ±7.4
3. Habitual barefoot, USA[1]	8 (7/1)	38.3 ±8.9	<2	1.80 ±0.07	77.2 ±13.3	8.3 ±4.1[1]
Adolescents						
4. Rural barefoot, Kenya	16 (8/8)	13.5 ±1.4	never	1.55 ±0.10	39.4 ±8.9	19.4[2] ±8.2
5. Urban shod, Kenya	16 (9/7)	15.0 ±0.8	<5	1.64 ±0.02	53.2 ±7.7	6.0[1] ±2.6[1]

[1]Among these runners, on average, 83% of training was in minimal shoes, 13% was barefoot, 4% was in cushioned, high-heeled running shoes.

[2]Estimated using average running speed, reported time spent running per day, and information provided by teachers.

Supplementary Data 3: Vibram FiveFinger™ Training Study

In order to test if and/or how habitually shod RFS runners change their strike when they transition from wearing running shoes to minimal footwear, we recruited 14 (10 male/4 female) subjects in 2008 and 2009 for a six week study. Subjects were solicited by email and word of mouth from the Harvard community. All subjects were habitual runners (>20 km run/week), with no lower limb or foot injuries. Average age was 21.4 years ± 1.8 s.d.; average weight was 68.3 kg ± 2.2 s.d.; average height was 170.1 cm ± 2.1 s.d.

Subjects were provided a pair of Vibram FiveFingers™ (FF, Sprint model) and asked to train for 6 weeks, keeping a log of their training. Subjects were asked to begin by running no more than 1.6 km/day in the FF shoes during the first week. They then increased the daily running distance by no more than 10-20% per week, to a maximum of 16-20 km/week. No subjects were paid, no subjects were instructed on how to run, and all gave their informed written consent as approved by the Harvard IRB.

Footstrike patterns were recorded prior to the study (Week 0) and at the end of the study (Week 6) using a high speed video camera (Fast-Tec Inline 500-M, San Diego, CA) at 500 Hz, and a Tekscan pressure pad (Tekscan HR Mat, South Boston, MA) at 250 Hz mounted along a 20 meter-long concrete floor trackway in the Peabody Museum (Harvard University, Cambridge, MA). Subjects were recorded for a minimum of 5 trials per condition to observe their modal footstrike pattern.

Kinematic results of these subjects (Supplementary Table 2, see Methods) showed that, on average, over the course of the 6 week training period the plantar angle of the foot at strike transitioned to being 7.2° ± 3.2 s.d. more plantarflexed ($p<0.05$), and average ankle angle at impact became more plantarflexed by 5.6° ± 3.6 s.d. ($p<0.05$).

Supplemental Data Table 2: Modal footstrike patterns among habitually shod runners who trained in Vibram FiveFinger® shoes

Strike Type	Week 0 (% subjects)	Week 6 (% subjects)
Rearfoot strike	72	36
Midfoot strike	14	0
Forefoot strike[1]	14	57
Toe strike[2]	0	7

[1]defined as a forefoot strike followed by heel contact (toe-heel-toe running)

[2]defined as a forefoot strike with no heel contact

Supplementary Data 4: Modelling collisional impulse in different foot strike types

In this supplement we derive the equations for a rigid plastic collision of a L-shaped object (thus similar to the lower leg and foot) that either has an ankle-like hinge at the corner, or has no joint (i.e., a stiff ankle). With respect to the collision, 'rigid' refers to the assumption that the collision is instantaneous, and thus gives rise to infinitely large instantaneous forces over an infinitesimal time period so that the net impulse due to the force is finite. Because the duration of the collision is nearly zero, the configuration of the system remains constant over the period of the collision. The term plastic refers to the assumption that there is no rebound. This supplement is in two parts: the first part considers the collision of a L-shaped bar, i.e. a double pendulum with a fused joint; and the second part considers the collision of a L-shaped double pendulum with a frictionless hinge joint. These conditions therefore represent the two extremes of ankle joint stiffness, infinite and zero, respectively.

Notation

Plain roman variables (e.g., A) denote labels for points in a figure, italicized variables (e.g., A) denote scalars, underlined variables (e.g., $\underline{A}$) denote vectors, and bold roman variables (e.g., **A**) denote matrices. Vector notation such as $\underline{A}_{P/O}$ refers to a vector quantity at point P, measured with respect to point O; examples include position or velocity of P with respect to O. Unreferenced vectors such as $\underline{A}_P$ are simply measured with respect to the origin. Angular momentum and inertia are always measured with respect to a point, and therefore their notation is of the type $\underline{A}_{/O}$ to indicate that that the vector $\underline{A}$ is defined with respect to a point O. Superscripts – and + denote the instant of

time before and after contact, respectively (e.g., $\underline{v}^+$). The point G refers to the centre of mass of the entire object. Finally, unit vectors of the global inertial coordinate system are denoted using $\hat{i}$, $\hat{j}$ and $\hat{k}$ for the x, y and z axes, respectively, such that the object is confined to the x-y plane.

Condition I: Infinitely stiff ankle joint

For simplicity, we consider first the case of an L-shaped bar falling vertically downward with velocity $\underline{v}_G^- = -v^-\hat{j}$ and no rotational velocity, i.e. $\underline{\Omega}^- = 0$. Because of the collision, there is an abrupt jump in the angular and linear velocities of the L-shaped bar to give $\underline{v}_G^+$ and $\underline{\Omega}^+ = \omega^+\hat{k}$. Figure S4.1 shows a free body diagram of the L-shaped bar with the "foot" part in contact with the ground at a point O (centre of pressure) that is located between the tip of the foot and the ankle. The only external force-impulse on the L-bar is applied at O. Therefore for the angular impulse-momentum balance about O, there are no external torque-impulses acting on the L-shaped bar about O, and hence the angular momentum $\underline{H}_{/O}$ about O is the same before and after the collision. In terms of the angular velocity vector $\underline{\Omega}$, the velocity of the centre of mass G is given by:

$$\underline{v}_G = \underline{v}_O + \underline{\Omega} \times \underline{r}_{G/O} \tag{S4.1}$$

and note that $\underline{v}_O^- = -v^-\hat{j}$ and $\underline{v}_O^+ = 0$. Then, the angular impulse-momentum balance is expressed as $\underline{H}_{/O}^+ = \underline{H}_{/O}^-$ where:

$$
\begin{aligned}
\underline{H}_{/O}^- &= (m+M)\underline{r}_{G/O} \times \underline{v}_G^- \\
\underline{H}_{/O}^+ &= (m+M)\underline{r}_{G/O} \times \underline{v}_G^+ + \mathbf{I}_{/G}\underline{\Omega}^+
\end{aligned}
\tag{S4.2}
$$

and m is the mass of the foot, M is mass of the shank, and $\mathbf{I}_G$ is the moment of inertia matrix of the foot plus shank about the centre of mass G, where only the principal inertia I_{zz} parallel to the z-axis is relevant for this planar object. Because the problem is

planar, the only non-zero component of the angular momentum vectors is the z-component, yielding one equation with one unknown, ω^+, which we can solve. We find $\underline{v}_G^+$ using equation S4.1 and linear impulse-momentum balance for the L-shaped bar gives us the impulse $\underline{J}$ at the contact point O as:

$$\underline{J} = (m + M)(\underline{v}_G^+ - \underline{v}_G^-) \tag{S4.3}$$

Therefore, the effective mass M_{eff} (equivalent to equation 2 from the main text) is given by:

$$M_{\text{eff}} = \left| \frac{\underline{J}.\hat{j}}{v^-} \right| \tag{S4.4}$$

By solving equations S2.2 to find ω^+, we find M_{eff} for a L-shaped bar (infinitely stiff ankle) that is falling vertically with a speed v^- as:

$$M_{\text{eff}} = \frac{l^2 m (m + 4M) + 4L^2 M (m + M)}{4 \left(l^2 \left(3s^2 (m + M) - 3ms + m \right) + L^2 M \right)} \tag{S4.5}$$

where s is the strike index (distance from the heel to the centre of pressure at impact relative to total foot length), L and l are the shank's and foot's length, respectively. For generating the graph of M_{eff} as a function of the strike index, s, we use the mean values reported by Dempster (1955) to set $m = 1.4\%$ body mass, $M = 4.5\%$ body mass, and $L = 1.53 \, l$.
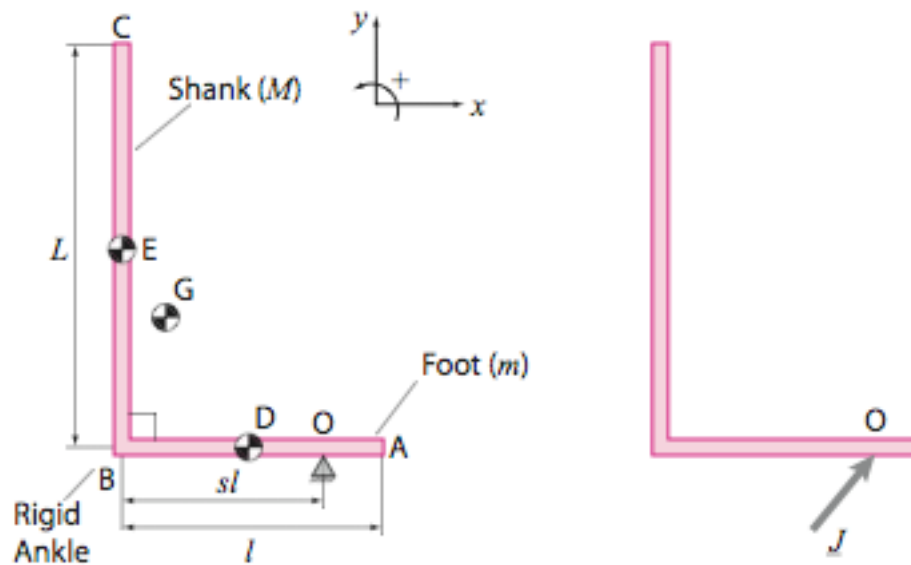
Supplementary Figure S4.1: A right angled L-shaped bar as a model of a foot plus shank having infinite ankle stiffness, and its free body diagram. In the collision free body diagram (right), only the impulse $\underline{J}$ due to the collision is shown because the impulse from gravitational forces vanishes in the limit of a rigid collision that happens instantaneously. We use angular impulse-momentum balance about the point O to find the jump in velocity of the L-shaped bar from the collision. Linear impulse-momentum balance is then used to find $\underline{J}$.

Condition II: Infinitely compliant ankle joint

Here we derive M_{eff} as a function of strike index, s, for conditions in which the corner of the L-shaped "bar" has a frictionless hinge, i.e. a double-pendulum with its joint flexed to 90° when it collides with the ground. This is analogous to an infinitely compliant ankle. Figure S4.2 shows the collision free body diagram for this posture of the double pendulum. We assume that, just before impact, the entire object is moving downward with speed v^- (i.e., $\underline{v}_D^- = \underline{v}_E^- = \underline{v}_G^- = -v^-\hat{j}$) and no angular velocity (i.e.,

$\underline{\Omega}_m^- = \underline{\Omega}_M^- = 0$). Assuming a rigid plastic collision, we use angular impulse-momentum balance of the entire double pendulum about the collision point O, and the shank segment (of mass M) about the hinge point B. The angular momentum vectors about O and B are given by:

$$
\begin{aligned}
\underline{H}_{m+M/O} &= \left(m\underline{r}_{D/O} \times \underline{v}_D + \mathbf{I}_{m/D}\underline{\Omega}_m\right) + \left(M\underline{r}_{E/O} \times \underline{v}_E + \mathbf{I}_{M/E}\underline{\Omega}_M\right) \\
\underline{H}_{M/B} &= M\underline{r}_{E/B} \times \underline{v}_E + \mathbf{I}_{M/E}\underline{\Omega}_M \\
\underline{v}_D &= \underline{v}_O + \underline{\Omega}_m \times \underline{r}_{D/O} \\
\underline{v}_E &= \underline{v}_O + \underline{\Omega}_m \times \underline{r}_{B/O} + \underline{\Omega}_M \times \underline{r}_{E/B}
\end{aligned}
\tag{S4.6}
$$

where subscripts m, M and m+M refer to the two segments separately or together, and the only relevant element of the matrices $\mathbf{I}$ is the principal moment of inertia I_{zz} parallel to the z-axis. Because there are no external torques on the body about the points O and B, the angular impulse-momentum equations are:

$$
\begin{aligned}
\underline{H}_{m+M/O}^+ &= \underline{H}_{m+M/O}^- \\
\underline{H}_{M/B}^+ &= \underline{H}_{M/B}^-
\end{aligned}
\tag{S4.7}
$$

Using the two non-zero z-components of the of the angular momentum vectors in equation S4.7 and with $\underline{v}_O^- = -v^-\hat{j}$, $\underline{v}_O^+ = 0$, we solve for the two unknown angular velocities of the segments $\underline{\Omega}_m^+ = \omega_m^+\hat{k}$ and $\underline{\Omega}_M^+ = \omega_M^+\hat{k}$ after the collision. Then, linear impulse-momentum balance of the entire system gives us the collisional impulse, $\underline{J}$, that is imparted at the point O as:

$$
\begin{aligned}
\underline{J} &= (m+M)(\underline{v}_G^+ - \underline{v}_G^-) \\
\underline{v}_G &= \underline{v}_O + \frac{m\underline{v}_D + M\underline{v}_E}{m+M}
\end{aligned}
\tag{S4.8}
$$

Therefore, M_{eff} for the vertical impulse due to the collision is given by:

$$
M_{\text{eff}} = \left|\frac{\underline{J}.\hat{j}}{v^-}\right| = \frac{m(m+4M)}{4\left(3s^2(m+M) - 3ms + m\right)}
\tag{S4.9}
$$

Equations S4.5 and S4.9 are graphed in Figure 3a of the main text. The model presented here can be extended by considering rebound, friction, more segments to account for the thigh, torso, and so on. A detailed treatise on rigid body collisions can be found in Chatterjee, 1997. But to our knowledge, there has been no systematic analysis in the literature of how the ground reaction impulse is affected by the strike index, i.e. the point of collision of the distal segment.
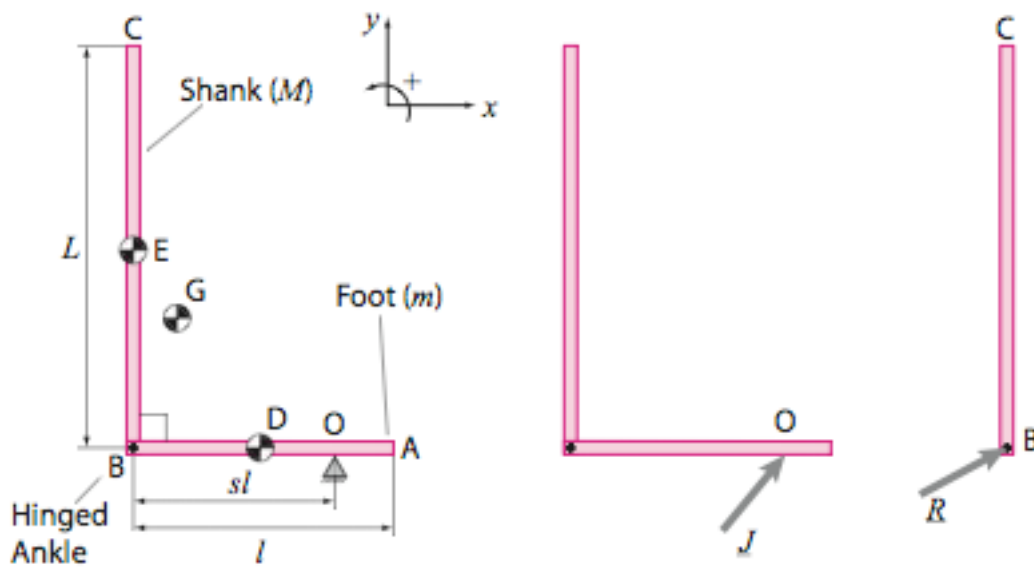
Supplementary Figure S4.2: A double pendulum with a frictionless hinge and 90° flexion as a model of a foot plus shank having infinite ankle compliance (zero stiffness), and the associated free body diagrams. We use angular impulse-momentum balance about O for the entire system, and balance about point B for the shank in order to find the jump in velocities arising from the collision. Gravitational impulses vanish in a rigid collision because it happens instantaneously. Finally, linear impulse-momentum balance for the whole system is used to calculate *J*.

References

1. Chatterjee, A. Rigid body collisions: some general considerations, new collision laws, and some experimental data. Ph.D. Dissertation. *Cornell University*, 1997.

2. Dempster, W.T. Space Requirements of the seated operator. *WADC-Technical Report 55-159*, Wright-Patterson Air Force Base, Ohio (1955).

Supplementary Data 5. Comparison of impact transient data and leg compliance in padded versus unpadded conditions

In order to assess the effect of substrate stiffness, rearfoot strike and forefoot strike runners (Groups 1 and 3 from Table 1) were tested on the same trackway described above with and without a 1 cm thick layer of carpet padding (Plushstep Deluxe 0.375 cm, 6 lbs/cft density, 4.2 psi tensile strength, 45% elongation). Variables measured were impact transient magnitude (in body weights), average rate of loading (from 200N to 90% of the impact transient peak), and overall leg compliance (hip marker drop over the period of the impact transient normalized by 90% of the impact transient magnitude).

Results, illustrated in Supplementary Figure 2, show that runners adjust leg stiffness depending on surface hardness in both the shod and barefoot conditions as demonstrated in previous studies of shod subjects (Feehery, 1986; Dixon et al, 2000). Although habitually shod rearfoot strikers had significantly higher rates of loading without padding than with padding in the barefoot condition ($p < 0.01$). However, their rates of loading when shod did not differ with or without padding. Additionally, their rates of loading were not significantly different from those of habitually barefoot forefoot strikers with or without padding (see main text). Habitual barefoot toe-heel-toe runners who forefoot strike actually had slightly lower (but not significantly different, $p = 0.34$) magnitudes of loading during impact on hard versus cushioned surfaces; they also experienced significantly higher rates of loading when shod versus unshod ($p < 0.05$).

These results therefore indicate that habitual barefoot runners who forefoot strike are not negatively affected by hard substrates, but instead have impact transient

characteristics that are similar or smaller than those experienced by shod runners under the same conditions.
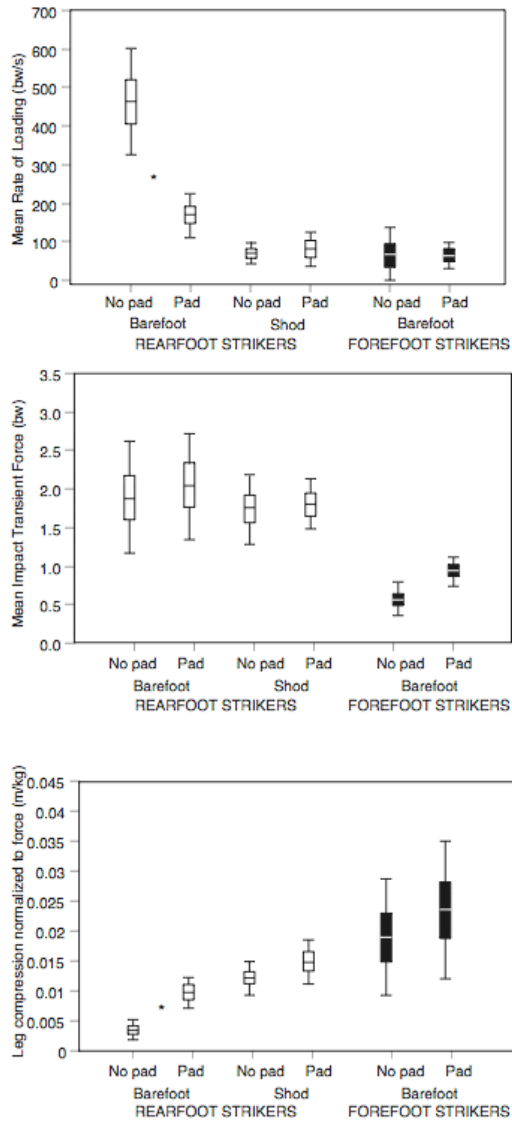
Supplementary Figure 2 Impact transient characteristics and overall leg compliance in padded versus unpadded conditions in habitual barefoot and shod runners (* indicates significant difference as determined by ANOVA).

Supplementary Data 6: Additional kinematic and anthropmetric information

1. Quicktime format movies of representative footstrikes:

-Movie 1: Adolescent Kalenjin female, habitually barefoot, unshod condition (forefoot strike)

-Movie 2: Adolescent Kalenjin male, habitually barefoot, unshod condition (forefoot strike)

-Movie 3: Adult Kalenjin runner, habitually barefoot until adolescence, unshod condition (forefoot strike)

-Movie 4: Adult Kalenjin runner, habitually barefoot until adolescence, shod condition (midfoot strike)

-Movie 5: Adolescent Kalenjin student, habitually shod, shod condition (rearfoot strike)

-Movie 6. Adolescent Kalenjin student, habitually shod, unshod condition (rearfoot strike)

-Movie 7: Pressure pad movie of forefoot strike (toe-heel-toe running)

-Movie 8: Pressure pad movie rearfoot strike (heel-toe running)

-Movie 9: Pressure pad movie of midfoot strike

2. Additional notes.

Running form prior to mid-1970s.

Empirical data on the prevalence of different footstrike patterns from long distance runners prior to the mid-1970s is difficult to obtain because most films and videos were made at insufficient speeds to capture the instant of foot strike precisely. Interviews with older runners and training manuals, however, all indicate that FFS running was the

predominant running style among middle and long distance runners. A typical summary of what was considered normal running style running from this era is exemplified by Fred Wilt's *How They Train 2nd Ed* (1973, Track and Field News, Los Altos, CA, pg 122): "The supporting phase beings with the forward foot beneath the body's center of gravity. The knee is bent as the outer border of the ball of the foot makes contact with the ground. Immediately thereafter the heel comes to the ground naturally, with no effort being made to prevent it from grounding. This applies to sprinting as well as middle and long-distance running."

Heel pad thickness. Examination by palpation of the foot indicates that habitually unshod subjects from Kenya (Group 4) had more calloused feet than age-matched habitually shod subjects (Group 5). Future study is necessary to measure the difference in callous and heel pad thickness. Additionally, habitual barefoot subjects informed us that they found the hard, dirt trackway (a dry dirt road) on which we recorded them a "very comfortable" and "easy" surface on which to run.

Incline. Footstrike patterns are variable depending not only on substrate hardness and texture, but also incline. Habitually shod runners typically FFS when running up an incline, and RFS when running on flat surfaces or down an incline. We have observed that habitual barefoot runners both in America and Kenya predominantly FFS when running downhill by increasing joint flexion of the knee and hip.